한국부식학회지
J. Corros. Sci. Soc. of Korea
Vol. 18 No. 3 Sept. 1989
〈研究論文〉

DISCHARGE CHARACTERISTICS OF THE NICKEL HYDROXIDE ELECTRODE IN 30% KOH

Young Jin Kim

Center for Electrochemical Systems and Hydrogen Research
238 Wisenbaker Engineering Research Center
Texas A & M University
College Station, TX 77843-3577

The discharge behavior of the nickel hydroxide electrode has been investigated in 30% KOH at 25°C. Two voltage plateaus are displayed on the discharge curve of C/20. It is shown that the impedance of the nickel hydroxide electrode increases with decrease of the discharge potential, The discharge behavior of the nickel hydroxide electrode has been investigated in 30% KOH indicating the reduction of the β-NiOOH to the β-$Ni(OH)_2$ by proton diffusion process and hence the electronic conductivity change of the nickel hydroxide electrode. Furthermore, the γ-NiOOH, produced by prolonged oxidation of the β-NiOOH in 30% KOH, discharges at a slightly lower potential than the β-$Ni(OH)_2$ that could result in the life-limiting factor of several alkaline electrolyte storage batteries using the nickel hydroxide electrode as the positive plate.

INTRODUCTION

A number of studies have been made of the electrochemical behavior of the nickel hydroxide electrode due to its application as the positive component which requires repeated charge/discharge cycling in the alkaline electrolyte storage batteries [1-4]. This nickel hydroxide electrode is also used as a water electrolyzer [5] and microelectrochemical transistors [6]. It is well known that the charge and discharge reaction of the nickel hydroxide electrode in the alkaline environment is

$$Ni(OH)_2 + OH^- \rightleftharpoons NiOOH + H_2O + e^-$$

The general reaction scheme of the structural characteristics of the nickel hydroxide electrode has been initially proposed by Bode et. al. [7] as follows:

$$\begin{array}{ccc} \alpha\text{-}Ni(OH)_2 & \rightarrow & \beta\text{-}Ni(OH)_2 \\ \downarrow\uparrow & & \downarrow\uparrow \\ \gamma\text{-}NiOOH & \leftarrow & \beta\text{-}NiOOH \end{array}$$

suggesting the α-$Ni(OH)_2$/γ-NiOOH and the β-NiOOH systems during reduction-oxidation processes.

It was reported that the disordered α-$Ni(OH)_2$ is precipitated as primary products during the electrochemical or chemical impregnation and that the ordered β-$Ni(OH)_2$ can be

obtained by ageing of such compounds in concentrated KOH solution [8-10]. The β-NiOOH can be regarded as deriving from the β-$Ni(OH)_2$ by a direct reaction removing one proton and one electron. The γ-NiOOH, which can be produced by prolonged oxidation of the β-NiOOH or from poorly crystallized α-$Ni(OH)_2$, is known to be a higher oxidation state of nickel (3.3-3.7) than the β-NiOOH [11].

Previous paper reported that hydrogen shifts open-circuit potential(OCP) of the nickel hydroxide electrode in the negative direction during discharge due to the transformation of the β-NiOOH to the β-$Ni(OH)_2$ by hydrogen oxidation and modifies the mechanical and/or structural properties of the nickel hydroxide electrode during charging in 30% KOH [12]. In this paper, experimental results of charge/discharge behavior , OCP behavior, and AC-impedance measurements are reported in order to understand the discharge characteristics of the nickel hydroxide electrode in 30% KOH at 25°C in an argon environment.

EXPERIMENTALS

The nickel hydroxide electrode was prepared by electrochemical deposition of $Ni(OH)_2$ on nickel foil substrate in $Ni(NO_3)_2$ solution. Details of the preparation of electrode and deposition processes have been described elsewhere [12]. The theoretical capacity was calculated to be approximately 20 mAh based on the one electron transfer reaction from the β-$Ni(OH)_2$ to the β-NiOOH. All electrodes were cycled three times at C/5 charge rate for 1 hour and at C/2 discharge rate to 1.0V (Zn/ZnO) in 30% KOH at 25°C before use in order to stabilize the electrode capacity. This nickel hydroxide electrode was examined by scanning electron microscope (SEM) and X-ray diffraction (XRD).

Analytical reagent grade KOH was used to prepare 30% KOH solution at 25°C in deionized water and a ultra-high purity argon gas was purged through this solution during experiment. The electrochemical cell consisted of a nickel hydroxide working electrode, a Pt counter electrode, and a Zn wire reference electrode (Zn/ZnO). The reference electrode was isolated from the test solution by means of a Luggin capillary.

The electrochemical measurements were made by using a EG&G Model 273 Potentiostat/Galvanostat and Model 5301A Lock-In-Amplifier with Model 5315 Preamplifier. Impedance experiment was carried out from 5 Hz to 100 KHz with M378 software and a 5 mV AC signal. The constant currents for charge or discharge were supplied by Keithley 220 Programmable Current Source.

RESULTS AND DISCUSSION

ANALYSIS BY SEM AND XRD

Figures 1-A, B, and C show the XRD patterns of β-$Ni(OH)_2$, β-NiOOH, and γ-NiOOH, respectively. These pattern characteristics are in good agreement with others [4, 13, 14]. There were lines of the characteristic of the β-$Ni(OH)_2$, when the β-$Ni(OH)_2$ was prepared by electrochemical impregnation and immersed in KOH solution, having 2θ angles of 19°, 32.9°, 38.4°, 59.2°, 63.1°, 70.4°, and 73°. The β-NiOOH was obtained from the nickel hydroxide electrode charged at C/10 for 12 hours in 30%

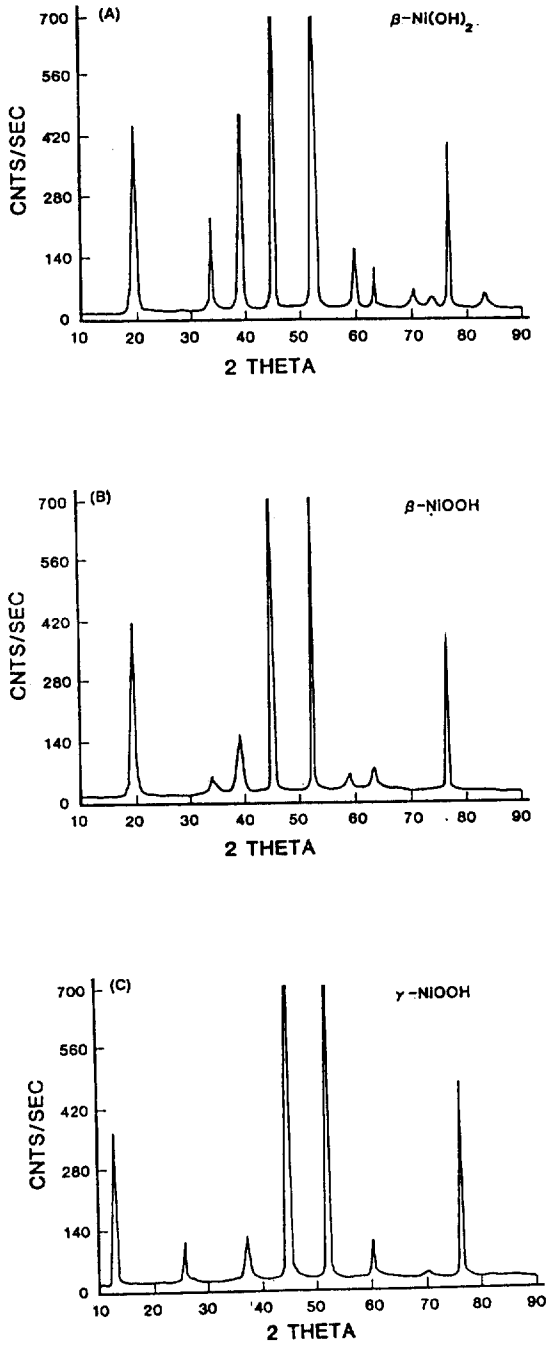

Fig. 1. X-ray diffraction patterns for : (A) as-impregnated, β-$Ni(OH)_2$, (B) after charge at C/10 for 12 hours, β-NiOOH, and (C) after overcharge at C/10 for 24 hours, γ-NiOOH.

KOH at 25°C. The XRD pattern of the β-NiOOH resembled the β-$Ni(OH)_2$ except that lines at 2θ = 32.9°, 38.4°, and 59.2° are reduced in intensity relative to the line at 19°. High charge rates and prolonged oxidation of the β-NiOOH are claimed to favor the formation of the γ-NiOOH. In this study, the γ-NiOOH was produced at a charge rate of C/10 for 24 hours in 30% KOH and XRD revealed 2θ angles of 12.8° and 26° with a total absence of the β-NiOOH lines.

The morphology of the surface layer of the nickel hydroxide electrode was examined by SEM. Figure 2 shows the surface layer of as-electrochemically impregnated nickel hydroxide electrode before use and one after 20 cycles (charge at C/10 for 12 hours and discharge at C/5 to 1.0V vs. Zn/ZnO in 30% KOH at 25°C). The difference on the surface layer between before and after cycles can be explained by the expansion of the nickel hydroxide active material. It was shown that data for molar volumes of divalent and of trivalent nickel hydroxides, measured in-situ, are given by Zimmerman et. al. as 3.3 g/cm^3 and 3.8g/cm^3, respectively [15]. Fritts [16] also reported a 5% change in volume during cycling. Furthermore, the unit cell dimensions are known to be changed from a=3.126Å and c=4.605Å for β-$Ni(OH)_2$ to a=2.82Å and c=4.85Å for β-NiOOH [13, 17] indicating the expansion/contraction of the nickel hydroxide active material during cycling, and the cell dimensions of a=2.82Å and c=20.65Å for γ-NiOOH can result in a large expansion along the c-axis. It was also reported that the nickel hydroxide electrode is the life-limiting component of the nickel-hydrogen battery due to the gradual expansion of the nickel hydroxide active material during charge/discharge cycling [18].

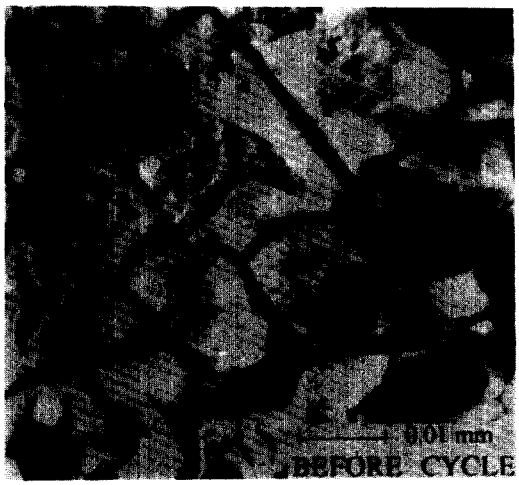

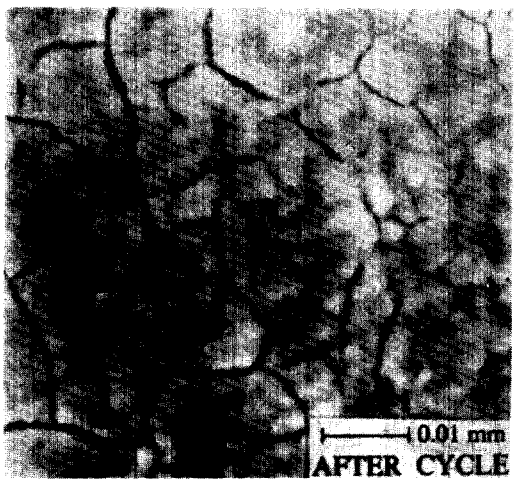

Fig. 2. SEM pictures of the surface morphology of the nickel hydroxide electrode before cycle and after 20 cycles in 30% KOH at 25°C.

ELECTROCHEMICAL CHARACTERISTICS

Figure 3 shows typical charge/discharge potential profiles as a function of time for the nickel hydroxide electrode; this electrode was first charged at C/10 for 12 hours to obtain the β-NiOOH and followed by discharge at C/20 to 1.0V in 30% KOH at 25°C. The slow discharge displayed two voltage plateaus. The AC-impedance measurement was carried out in order to understand the discharge kinetics of the nickel hydroxide electrode. Since impedance is sensitive to the applied potential and the applied time, spectra were measured after the electrode had been equilibrated at the desired potential. Figure 4 shows typical Bode plot of log frequency versus log resistance during the course of a C/20 discharge. The nickel hydroxide electrode has been held at different potentials for 1 hour in 30% KOH at 25°C. The impedance of the electrode increased with decrease of the discharge

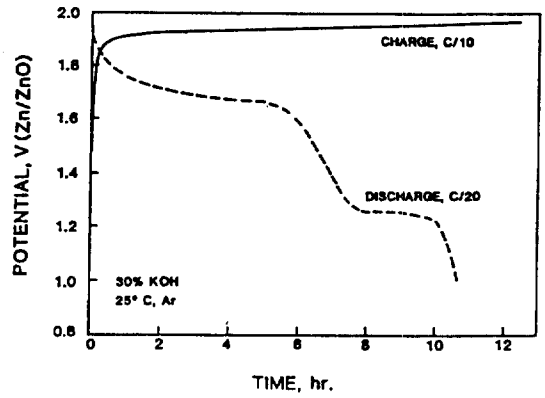

Fig. 3 Charge/discharge behavior as a function of time for the nickel hydroxide electrode in 30 % KOH at 25°C.

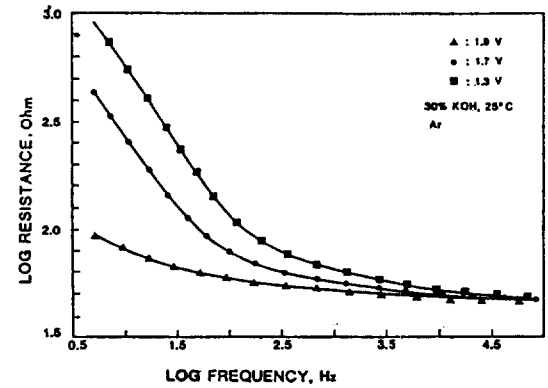

Fig. 4. Log frequency vs. log resistance of the nickel hydroxide electrode charged at different potential in 30% KOH at 25°C.

potential. This increase in impedance suggests a decrease in the state of charge due to the partial transformation of the conductive β-NiOOH to the less conductive β-$Ni(OH)_2$, which was ascertained by Nyquist plot of impedance shown in Figure 5.

It is, therefore, clear that the C/20 discharge curve would involve different processes that can control the reduction rate at the nickel hydroxide electrode. The reaction kinetics at 1.9V may be attributed to proton diffusion represented by a straight portion of the semicircular impedance plot. The diffusion of protons at the electrode/electrolyte interface and the charge transfer process may occur as follows;

$$H_2O \rightleftharpoons OH^- + H^+$$

$$NiOOH + H^+ + e^- \rightleftharpoons Ni(OH)_2$$

Previous study showed that this proton diffusion is predominantly along grain boundaries at the beginning of discharge [19]. While at 1.7V, another process, as well as the Warburg impedance term, begins to control the kinetics. Discharge at 1.7V increases the charge transfer resistance of the nickel hydroxide active material due to the partial transformation of β-NiOOH to β-$Ni(OH)_2$. Continuous discharge on the lower voltage plateau (1.3V) causes the decrease of electronic conductivity and/or the formation of poorly conductive layer on the interface between the nickel substrate and the nickel hydroxide active material.

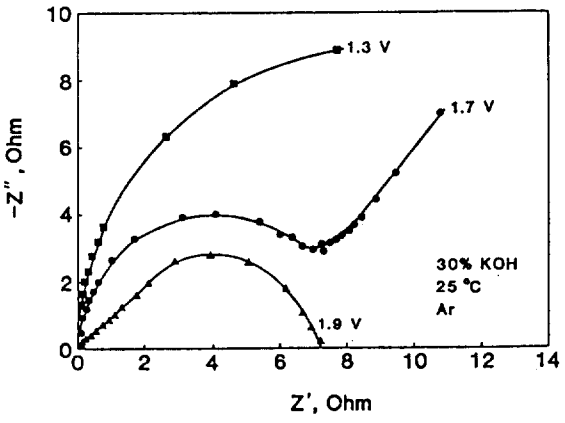

Fig. 5. Nyquist plot of the nickel hydroxide electrode at different potential in 30% KOH at 25 °C.

It was explained that the upper voltage plateau is controlled by the proton diffusion within the active material and the lower plateau controlled by the resistance of poorly conductive material formed on the interface [19, 20]. But, Barnard et. al [2] claimed that the lower voltage plateau is ascribed to the conductivity change of the nickel hydroxide active material and not to the formation of some new phase. In this study, the discharge characteristics of the C/20 curve can be explained by the proton diffusion at the upper plateau and decrease in conductivity of the active material by the formation of β-$Ni(OH)_2$ at the lower plateau voltage. However, the more careful studies are needed to understand the discharge kinetics of the nickel hydroxide electrode.

STRUCTURAL EFFECT

As mentioned before, prolonged oxidation of the β-NiOOH yields the γ-NiOOH. This can be facilitated with increase of KOH concentration [14]. Figure 6 shows typical discharge curves for the β-NiOOH and the γ-NiOOH in 30% KOH at 25°C. The β-NiOOH was obtained by charging at C/10 for 12 hours in 30% KOH and the γ-NiOOH by overcharging at C/10 for 24 hours. The nickel

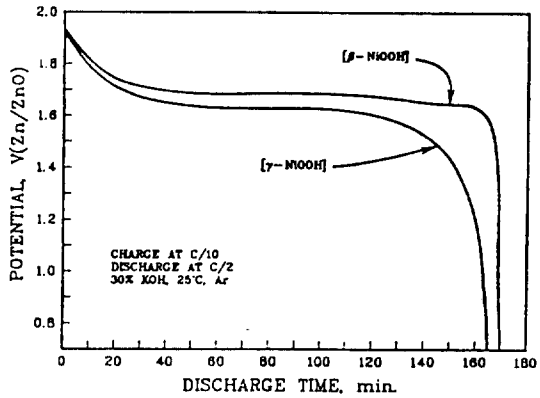

Fig. 6. Effect of crystalline phase of the nickel hydoxide electrode on the discharge behavior in 30% KOH at 25°C.

hydroxide electrode containing predominantly γ-NiOOH shows the lower discharge potentials than that with β-NiOOH. Also, the γ-NiOOH developed the lower OCPs, as shown in Figure 7. There was, however, no significant difference on the charge potential behavior.

It was shown that the discharge potential of the γ-NiOOH is slightly lower than that of the β-NiOOH [21]. This potential separation between the γ-NiOOH and the β-NiOOH was explained by a consequence of the different stand-

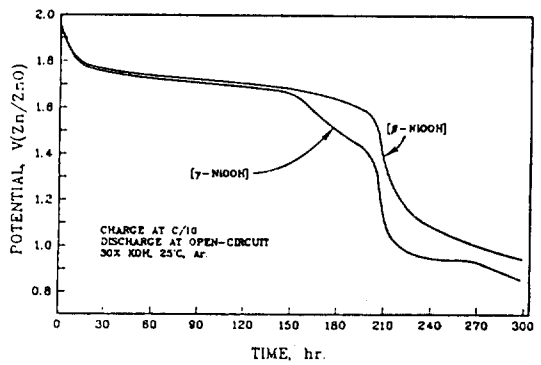

Fig. 7. Effect of crystalline phase of the nickel hydroxide electrode on the open-circuit potential behavior in 30% KOH at 25°C.

ard potentials for the α-$Ni(OH)_2$/γ-NiOOH and the β-$Ni(OH)_2$/β-NiOOH systems, respectively [22], and they also have found that the γ-NiOOH phase reveals efficient high-rate discharge. It was also reported that the excessive overcharging for the formation of a higher degree of the γ-NiOOH accelerated the failure of the nickel hydroxide electrode in KOH electrolyte [23, 24]. However, both Tuomi [14] and Harivel [23] have claimed that the discharge efficiency of the γ-NiOOH is poor, and therefore that it only undergoes substantial discharge at low rates. As shown in Figures 6 and 7, it is clear that the γ-NiOOH produces the lower capacity which results in the life-limitation of the nickel hydroxide electrode as the positive component such as Ni-Cd, Ni-Fe, Ni-Zn and Ni-H_2 batteries.

CONCLUSION

The discharge characteristics of the nickel hydroxide electrode have been investigated in 30% KOH at 25°C. It was found that the impedance increases with decrease of the discharge potential suggesting the reduction of the β-NiOOH to the β-$Ni(OH)_2$ by proton diffusion process and hence the decrease in electronic conductivity of the nickel hydroxide active material. In addition, the excessive overcharge of the nickel hydroxide electrode lowers the discharge potentials and OCPs due to the degradation of the nickel hydroxide electrode by a higher degree of the γ-NiOOH which causes the decrease in capacity of the nickel hydroxide electrode during charge/discharge cycling.

REFERENCES

1. S.U Falk and A.J. Salkind, *"Alkaline Storage Batteries,"* John Wiley & Sons, Inc., New York (1969).
2. R. Barnard, G.T. Crickmore, J.A. Lee, and F. L. Tyle, J. Appl. Electrochem., **10**, 61 (1980).
3. B. E. Conway and M.A. Satter, J. Electroanal. Chem., **19**, 351 (1968).
4. G.W.D. Briggs, *"A Specialist Periodical Report: Electrochemistry, V-4,"* The Chemical Society, London (1974).
5. P.W.T Lu and S. Srinivasan, J. Electrochem. Soc., **125**, 1416 (1978),
6. M. J. Natan, D. Belanger, M.K. Carperter, and M.S. Wrighton, J. Phys. Chem., **91**, 1835 (1987).
7. H. Bode, K. Dehmelt, and J. Witte, Electrochim. Acta, **11**, 1079 (1966).
8. D. Bango and J. Longuet-Escard, J. Chim. Phys., **51**, 215 (1954).
9. E. Suoninen, T. Juntunen, H. Juslen, and M. Pessa, Acta Chem. Scand., **27**, 2013 (1973).
10. P. Oliva, J. Leonardi, J. F. Laurent, C. Delmas, J. J. Braconnier, M. Figlarz, and F. Frevet, J. Power Sources, **8**, 229 (1982).
11. O. Glemser and J. Einerhand, Z. Anorg. All. Chem., **261**, 26 (1950).
12. Y. J. Kim, S. Srinivasan, and A. J. Appleby, J. Appl. Electrochem., in press.
13. S.U. Falk, J. Electrochem. Soc., **107**, 661 (1960).
14. D. Tuomi, J. Electrochem. Soc., **112**, 1 (1965).
15. A. H. Zimmerman and P. K. Effa, Extended Abstracts of the Electrochemical Soc., *V-85(2)*, Abstract. No. 28, (1985).
16. D. H. Fritts, J. Electrochem. Soc., **129**, 118 (1982).
17. A. J. Salkind, P. F. Bruins, J. Electrochem. Soc., **109**, 358 (1962).
18. H. S. Lim, *"Long Life Nickel Electrodes for Nickel-Hydrogen Batteries,"* NASA-CR-174815, December (1984).
19. A. H. Zimmerman, J. Power Sources, **12**, 223 (1984).
20. D.M. MacArther, J. Electrochem. Soc., **117**, 422, 729 (1970) .
21. N. Yu Uflyand, A. M. Novakovskii, and S.A. Rozentsveig, Elektrokhimiya, **3**, 537 (1967).
22. R. Barnard, C. F. Randell, and F.L. Tyle, J. Appl. Electrochem., **10**, 109 (1980).
23. J. P. Harivel, *"Power Sources,"* Edited by D. H. Collins, Oriel Press, Newcastle-Upontyne, pp. 239 (1966).
24. D. M. MacArther, *"Power Sources,"* Edited by D. H. Collins, Oriel Press, Newcastle-Upontyne, pp. 91 (1970).